Wettability and flotation of etched ultra high molecular weight polyethylene fibres

M. S. Silverstein* and O. Breuer
Department of Materials Engineering, Technion — Israel Institute of Technology, Haifa 32000, Israel
(Received 11 June 1992; revised 2 November 1992)

The use of ultra high molecular weight polyethylene (UHMW-PE) fibres in composite materials is limited by their poor adhesion to the matrices. The wetting of the fibre is an integral step in the adhesion process but the extent of fibre wetting is often difficult to establish. Both surface roughness and surface polarity contribute to fibre wettability. A flotation method has been used to study the wettability of chemically etched UHMW-PE fibres. The flotation is defined by the percentage of fibres that float on a liquid flotation medium. The dependence of flotation on surface tension exhibits a float/sink transition that can be used to characterize the effects of surface roughness and surface oxidation. Chromic acid removes an oxygen-rich skin on the as-received fibre surface, increases surface roughness and oxidizes the UHMW PE yielding an increase in apparent surface tension.

(Keywords: UHMW-PE; etching; flotation; fibres; wettability; surface tension)

INTRODUCTION

Polyethylene fibre surface modification

Extended chain ultra high molecular weight polyethylene (UHMW-PE) fibres are one of the more advanced polymer fibres in the high performance fibre field[1]. The greatest drawback to using these ultra high strength and stiffness fibres in composite material applications has been their poor adhesion to polymer matrices. Several methods of fibre surface treatment including chemical etching and plasma etching have been used in an attempt to improve adhesive bonding[2–4].

The modification mechanism in chemical etching consists of the abstraction of hydrogen atoms from the polymer backbone and their replacement with polar groups. The polar groups introduced on the fibre surface by etching should increase the surface tension and enhance wetting. These polar groups may also present possible sites for chemical reactions with the matrix resin. The Wenzel equation predicts that an increase in surface roughness may yield an increase in apparent surface tension[5].

Surface modification through chromic acid, potassium permanganate ($KMnO_4$) and hydrogen peroxide (H_2O_2) etching have been studied. The surface oxygen content was characterized through a combination of electron spectroscopy for chemical analysis (e.s.c.a.) and Fourier transform infra-red spectroscopy (*FT*i.r.)[6]. Scanning electron microscopy (SEM) has revealed changes in surface morphology and in failure mechanism for the etched fibres[7]. The epoxy–fibre interfacial shear strength was characterized through the debonding of epoxy droplet microbonds[2].

Surface wettability

An integral step in the adhesion process is the wetting of the polymer substrate. Polymer wettability can be reflected by polymer–adhesive interfacial tension. The contact angles between a droplet of adhesive and a planar polymer substrate are commonly used to determine polymer surface tension and interfacial tension[5]. The interpretation of the contact angle on fibres tens of micrometers in diameter, however, is much more complex with no analytical solution[8]. The wettability of both carbon and UHMW-PE fibres has been characterized using a contact angle technique with a graphical or iterative solution[9,10].

Fibre flotation

A different approach to assessing wettability is based on the flotation of small specimens such as spherical beads[11]. Two miscible liquids of different surface tensions and of densities less than that of the specimen are chosen as the flotation medium. The liquids are chosen such that in one the sample floats and in the other the sample sinks. A transition from floating to sinking will occur at some intermediate composition. In an application of this technique the rest position (no external forces present) of a floating sphere was described with a force balance. The point of instability, the float/sink transition, was derived yielding the contact angle as a function of the radius and density of the spheres and of the surface tension and density of the solution at the float/sink transition. The surface tension of the solid was calculated once the contact angle was determined[11].

In this research the flotation method is used to characterize the effects of chemical etching on the wettability of UHMW-PE fibres by applying the technique developed for spheres to cylinders.

* To whom correspondence should be addressed

0032-3861/93/163421-07

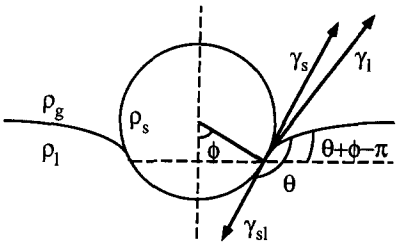

Figure 1 Rest state of a solid cylinder at a fluid interface. γ_{sl} is the solid–liquid interfacial tension

THEORY

Force balance on a cylinder

The net force on a solid cylinder at a liquid interface, as schematically illustrated in *Figure 1* (after Rapacchietta *et al.*[12]), can be determined analytically using a force balance (assuming that end effects are negligible). The vertical forces in this balance are the weight, the buoyancy and the surface tension[12]. The contact angle (θ) and the angle which locates the three-phase line on the solid surface (ϕ) are used to define the position of the cylinder in the liquid.

A normalized radius (R_n) based on the cylinder radius (R), liquid surface tension (γ_l, liquid/air), liquid density (ρ_l) and gravitational acceleration (g) is defined in equation (1). A normalized density (ρ_n) is defined in equation (2) assuming that the density of the gas phase (ρ_g, air) is insignificant compared to the liquid and solid densities (ρ_l and ρ_s, respectively). The net force (F_n) in equation (3) is therefore determined[12] by four system properties R_n, ρ_n, ϕ and θ. The F_n in equation (3) can be calculated as a function of ϕ for a given θ in a system for which R_n and ρ_n are known.

$$R_n^2 = \frac{\rho_l g}{\gamma_l} R^2 \tag{1}$$

$$\rho_n = \frac{\rho_s}{\rho_l} \tag{2}$$

$$F_n = 2\sin(\theta+\phi) + R_n^2(\pi\rho_n - \phi + \sin\phi\cos\phi) + \mathrm{sgn}(180-\phi-\theta)R_n\sqrt{8}\sin\phi\sqrt{[1+\cos(\phi+\theta)]} \tag{3}$$

The stability of the cylinder's state is indicated by the derivative of F_n with respect to ϕ, $\partial F_n/\partial\phi$, in equation (4). The value of ϕ at constant θ for which $F_n = 0$ and $\partial F_n/\partial\phi \leqslant 0$ is the position at which the cylinder is floating at rest, i.e. the F_n on the floating cylinder is zero. This point corresponds to a minimum in an equivalent energy balance for this system. The state $F_n = 0$ and $\partial F_n/\partial\phi > 0$ is unstable and corresponds to an energy maximum. Additionally, if $F_n > 0$ for all ϕ the cylinder has no stable floating position and will sink.

The transition from floating to sinking for a given θ for a cylinder at rest ($F_n = 0$) can be found by setting both F_n and $\partial F_n/\partial\phi$ equal to zero. The contact angle can be calculated from the system of two equations [equations (3) and (4)] and two unknowns (θ and ϕ) given R_n and ρ_n at the float/sink transition. The solid surface tension (γ_s, really solid/vapour) can be calculated from equation (5) once the contact angle and liquid surface tension at the float sink transition have been determined.

The liquid properties are defined by the composition of the flotation medium at which the float/sink transition occurs in a series of solutions. These properties are used to calculate the surface tension of the solid.

$$\frac{\partial F_n}{\partial\phi} = 2\cos(\phi+\theta) - 2R_n^2\sin^2\phi + ([\mathrm{sgn}(180-\phi-\theta)R_n]/\{\sqrt{[1+\cos(\phi+\theta)]}\} \times \{\sqrt{8}\cos\phi[1+\cos(\phi+\theta)] - \sqrt{2}\sin\phi\sin(\phi+\theta)\}) \tag{4}$$

$$\gamma_s = \tfrac{1}{4}(1+\cos\theta)^2\gamma_l \tag{5}$$

EXPERIMENTAL

Materials

The UHMW-PE ($M_w = 1.5\times10^6$) fibre was a 120 filament Spectra-1000 fibre tow of 650 denier (g per 9000 m) supplied by Allied Fiber Inc., VA, USA. The chromic acid etching solution was prepared by mixing potassium dichromate (IV) ($K_2Cr_2O_7$), sulfuric acid (H_2SO_4) and distilled water in a mass ratio of 7:150:12. The $KMnO_4$ etching solution was prepared by mixing aqueous 0.2 M $KMnO_4$ with aqueous 0.2 M nitric acid (HNO_3) in a 4:1 ratio. The H_2O_2 etching solution was 30% H_2O_2 in water. The flotation media consisted of analytical n-propylamine (nPA) ($\gamma_l = 22.4\,\mathrm{mN\,m^{-1}}$, $\rho_l = 720\,\mathrm{kg\,m^{-3}}$) and distilled water ($\gamma_l = 73.1\,\mathrm{mN\,m^{-1}}$, $\rho_l = 1000\,\mathrm{kg\,m^{-3}}$).

Chemical etching

The fibres were separated from the tow and left in the etching solutions at room temperature for 4 h. After etching the fibres were first washed in running distilled water and then in ethanol. The fibres were dried in a vacuum oven at room temperature for 12 h.

Surface characterization

Surface oxygen content was measured through e.s.c.a. with a resolution of 25 eV. SEM of gold-coated fibres was carried out at 15 kV.

Fibre flotation

The flotation technique apparatus is schematically illustrated in *Figure 2*. The as-received and etched fibres were cut into 1 cm lengths for flotation. The flotation media consisted of aqueous nPA solutions. The volumetric composition of nPA was varied from 0 to 100% at 10% intervals. A flotation solution was placed

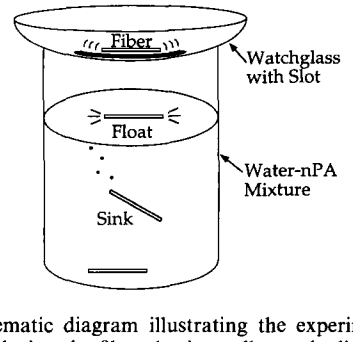

Figure 2 Schematic diagram illustrating the experimental flotation technique for placing the fibres horizontally on the liquid surface

in a beaker such that the beaker was almost filled. The beaker was covered with a watch-glass which had at its centre a slot ~3 cm in length and 3 mm in width. The UHMW-PE fibre was placed on the watch-glass, aligned with the slot, and gently rolled through the slot into the beaker. The fibre flotation for a given flotation medium was taken as the percentage of fibres that float on the surface from a sample of >100 fibres.

Density and surface tension

The densities of the flotation media were calculated using the rule of mixtures and verified using a pycnometer. The surface tensions of the flotation media were determined using the du Nuouy ring technique.

RESULTS AND DISCUSSION

Float/sink transition — larger radii

The force balance diagram in *Figure 3a* (F_n as a function of ϕ for various values of θ, after Rapacchietta *et al.*[12]) has $R_n = 1.67$ ($R_n^2 = 2.8$) and $\rho_n = 1.25$. These parameters correspond to a cylinder diameter of 3.2 mm arbitrarily assuming a typical liquid surface tension of 30 mN m^{-1} and a typical liquid density of 860 kg m^{-3}. The float/sink transition calculated from equations (3) and (4) occurs at $\theta = 64.06°$ and $\phi = 163.92°$.

A significant change in the force diagram occurs when the value of the normalized radius decreases. The net force diagram in *Figure 3b* for $R_n = 0.53$ ($R_n^2 = 0.28$) and $\rho_n = 1.25$ has no discernible float/sink transition. These parameters correspond to a cylinder radius of 1.0 mm assuming $\gamma_l = 30$ mN m^{-1} and $\rho_l = 860$ kg m^{-3}. There is no float/sink transition, no zero/minimum net force coincidence for the smaller radii. Different conditions must be used to describe a float/sink transition for cylinders of smaller radii.

Float/sink transition — smaller radii

The changes in the net force diagram become even more pronounced at very small R_n. The net force diagram in *Figure 3c* is for $R_n = 10^{-2}$ ($R_n^2 = 10^{-4}$) and $\rho_n = 1.25$, corresponding to a cylinder radius of 19 μm assuming $\gamma_l = 30$ mN m^{-1} and $\rho_l = 860$ kg m^{-3}. The absence of the zero/minimum coincidence in *Figure 3c* is strikingly obvious. The intersections with zero net force occur when $(\phi + \theta) = 180°$ (excluding the additional unstable state intersections for $\theta = 180°$ and for $\theta = 0°$). All the minima in the net force occur when $(\phi + \theta) = 270°$.

The dependence of the different terms in the force balance in equation (3) on normalized radius determines their magnitudes and yields the relationship between ϕ and θ seen in *Figure 3c*. The first term [equation (6)] is independent of R_n, the second term [equation (7)] depends on R_n and the third term [equation (8)] depends on R_n^2. Both the second and third terms become negligible as R_n decreases. Equation (6) dominates equation (3) at small values of R_n yielding the net force diagram in *Figure 3c*. The F_n in equation (3) for small values of R_n approaches zero when $\sin(\phi + \theta)$ approaches zero [$(\phi + \theta)$ approaches 180°]. The F_n for small values of R_n approaches a minimum from equation (4) when $\cos(\phi + \theta)$ approaches zero [$(\phi + \theta)$ approaches 270°]. The minimum and zero net force never coincide under these

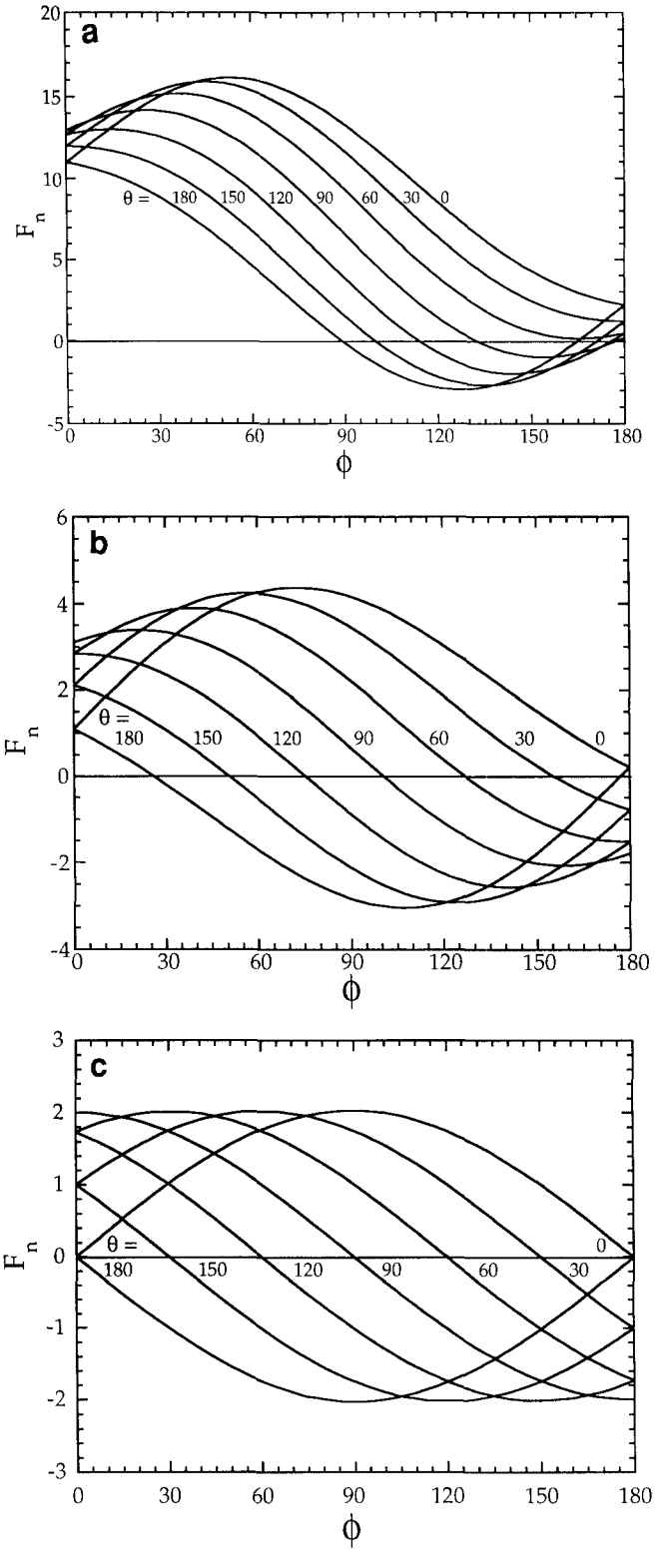

Figure 3 Variation of net force with ϕ for different values of θ given $\rho_n = 1.25$ and an R_n of: (a) 1.675; (b) 0.53; (c) 10^{-2}

conditions.

$$2\sin(\theta + \phi) \tag{6}$$

$$\sin(180 - \theta - \phi)R_n\sqrt{8}\sin\phi\sqrt{1 + \cos(\theta + \phi)} \tag{7}$$

$$R_n^2(\pi\rho_n - \phi + \sin\phi\cos\phi) \tag{8}$$

The dependence of equation (3) on R_n has several other ramifications at small values of R_n where there is no significant dependence of F_n on normalized radius. The

net force diagrams for $R_n = 10^{-3}$ and 10^{-4} are practically identical to *Figure 3c*. In addition, there is no significant dependence of F_n on normalized density. The net force diagrams for $\rho_n = 1.01$ and 5 are also practically identical to *Figure 3c*.

Float/sink condition

The establishment of a float/sink transition, the conditions under which cylinders sink, is of significance for cylinders with micrometer scale diameters. One possible condition would be that the float/sink transition for small radii occurs when the cylinder is completely enveloped in the liquid, when ϕ approaches 180°. The sinking phenomenon changes from one established by the coincidence of a zero and minimum net force to one established by cylinder envelopment at high values of ϕ with decreasing R_n. The simplest assumption to make would be that this transition occurs at $\phi = 180°$. Given the relationship established between ϕ and θ at small values of $R_n[(\phi + \theta) = 180°]$, the float/sink transition occurs at $\theta = 0°$. In other words, as shown by the rest positions in *Figure 3c*, the cylinder floats for all values of θ until θ reaches zero, at which point the cylinder is entirely wet by the liquid. This point of total envelopment is considered the float/sink transition. The surface tension of the solid cylinder (γ_s) can be calculated using equation (5) given θ; assuming $\theta = 0°$ yields $\gamma_s = \gamma_l$.

The envelopment of the cylinder may actually occur at lower values of ϕ. If the bulging menisci touch at $\phi \geqslant 160°$ the physical configuration established by the force balance is changed[12]. The touching menisci would envelop the cylinder with liquid and thus cause the fibre to sink. An equally valid float/sink transition assumption in light of the meniscus effect would be at $\phi = 160°$ (and $\theta = 20°$); assuming $\theta = 20°$ yields $\gamma_s = 0.94\ \gamma_l$. The approximations used in deriving the float/sink equations and the breadth of the experimentally determined transitions restrict the use of this tool to comparative analyses. A float/sink transition definition at $\phi = 180°$ will be used in this work in light of the qualitative nature of the data interpretation.

UHMW-PE fibre surfaces

The average radius of the irregularly shaped UHMW-PE fibres is 14 μm. The force balance for these fibres can be approximated by equation (6) and described by *Figure 3c*. The fibre surfaces have been characterized using several different techniques. Two of the most significant parameters evaluated were surface oxygen content and surface roughness[6]. The as-received fibre exhibits the smooth surface seen in *Figure 4a*. The fibrillar nature of the UHMW-PE fibre is revealed after 4 h etching in chromic acid in *Figure 4b*. Chromic acid was the most powerful etchant used and the chromic acid etched fibre

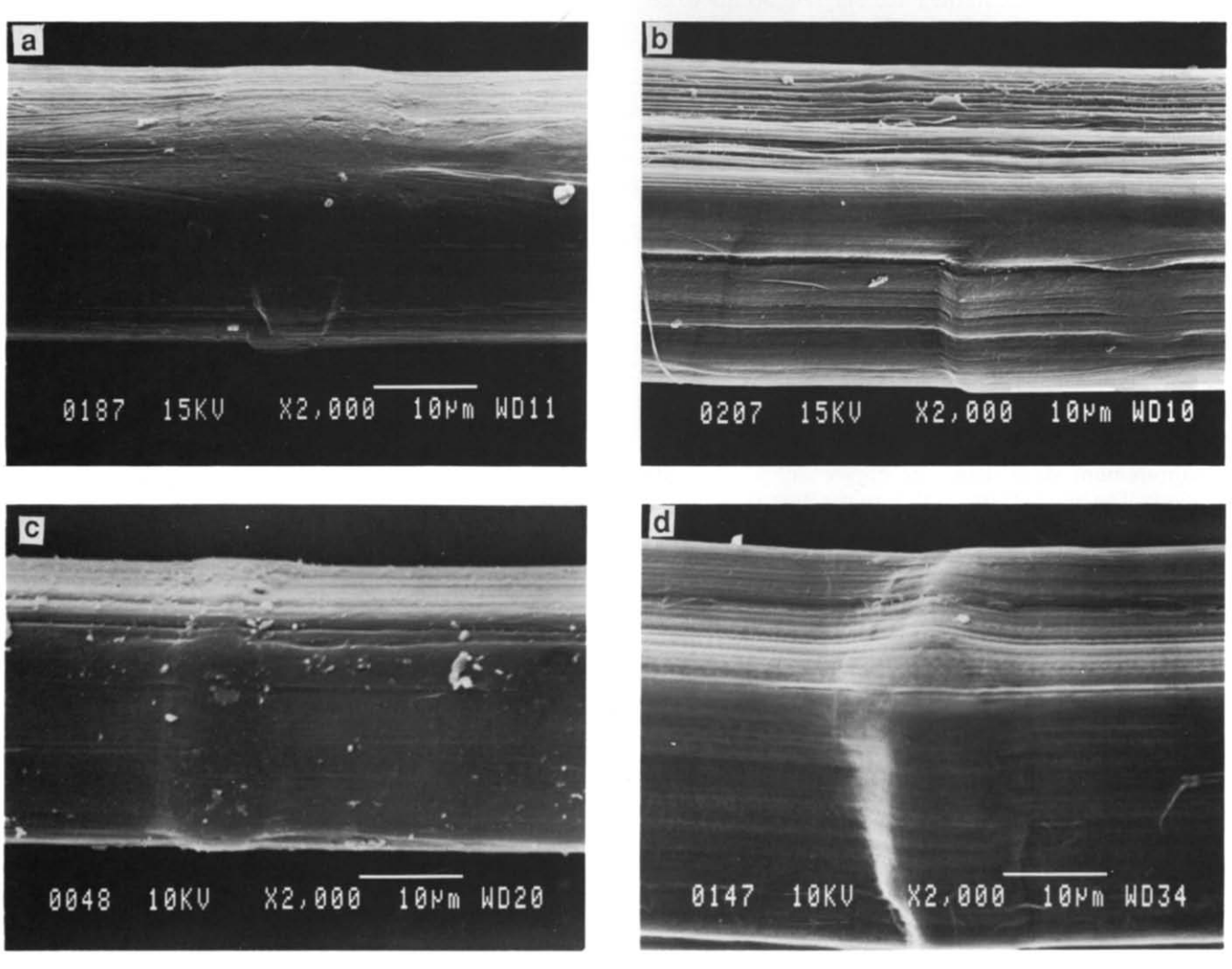

Figure 4 Scanning electron micrographs of UHMW-PE fibres: (a) as-received; (b) chromic acid etched; (c) $KMnO_4$ etched; (d) H_2O_2 etched

has the roughest surface. Etching for 4 h in $KMnO_4$ or H_2O_2 does reveal fibrillar surfaces, as seen in *Figures 4c* and *d*, respectively.

The original intent of etching was to introduce polar groups on the surface of non-polar UHMW-PE. The surprisingly high surface oxygen content for the as-received fibres in *Table 1* reflects the existence of an oxygen-rich skin formed by oxidized low molecular weight fragments and solvent excluded during crystallization[2]. Washing the fibres cannot remove this skin layer. Etching the oxygen-rich as-received fibre for 4 h in chromic acid, $KMnO_4$ or H_2O_2 at room temperature reduces the surface oxygen content in *Table 1*.

The oxygen on the surface of the chromic acid etched fibres, where the etching is highly efficient, may be associated with oxidized UHMW-PE. Most of the oxygen on the $KMnO_4$ etched fibres is associated with manganese dioxide particles precipitated during etching and seen in *Figure 4c*[6]. The small amount of oxygen remaining on the $KMnO_4$ and H_2O_2 fibre surface may be associated with remnants of the skin layer. The surface oxygen and nitrogen contents were not altered by the immersion of the fibres in nPA.

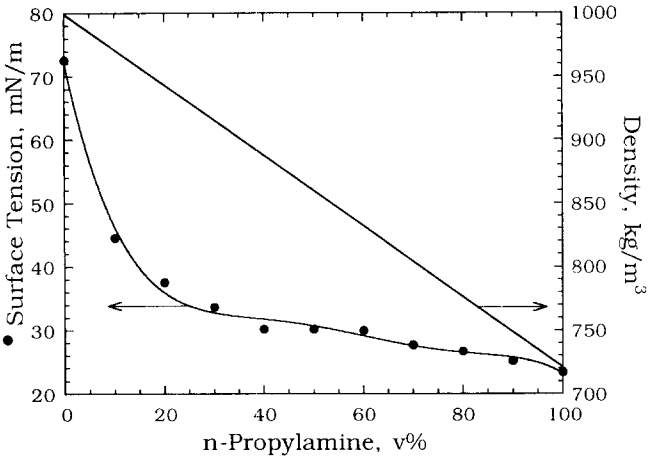

Figure 5 Variation of surface tension and density of water–nPA flotation media with composition

Flotation of UHMW-PE fibres

The variation of the flotation medium's density and surface tension with nPA content is seen in *Figure 5*. The density in *Figure 5* was calculated using the rule of mixtures and verified experimentally. The surface tension shows a sharp decrease from 0 to 10% nPA and a decreasing rate of change with increasing nPA content thereafter. The vertical line on this graph and on the flotation diagrams indicates 11% nPA ($\gamma_l = 45\ mN\ m^{-1}$), the composition for which the liquid and solid densities are equal. Experimental points at nPA concentrations of $< 11\%$ are of no significance to the establishment of a float/sink transition since the fibres cannot sink.

The flotation diagrams (after Marmur *et al.*[11]) for the as-received fibres and fibres etched for 4 h in chromic acid, $KMnO_4$ and H_2O_2 are in *Figures 6a–d*, respectively. The as-received, chromic acid etched and $KMnO_4$ etched fibres (*Figures 6a–c*) all exhibit a similarly shaped curve. There is a steep decrease from 100% flotation to between 70% and 50% flotation, a plateau between 70% and 50% flotation, and then a steep decrease to 0% flotation. The H_2O_2 etched fibres, on the other hand, exhibit an initially gradual decrease from 100% flotation that becomes continually steeper in *Figure 6d*.

Table 1 Surface oxygen content of UHMW-PE fibres

Etch	Time (h)	O (at%)
None	–	21.9
Washed	–	22.2
$K_2Cr_2O_7$	4	13.5
$KMnO_4$	4	16.5 (5.4)[a]
H_2O_2	4	6.6

[a] The value in parentheses is for Mn (at%)

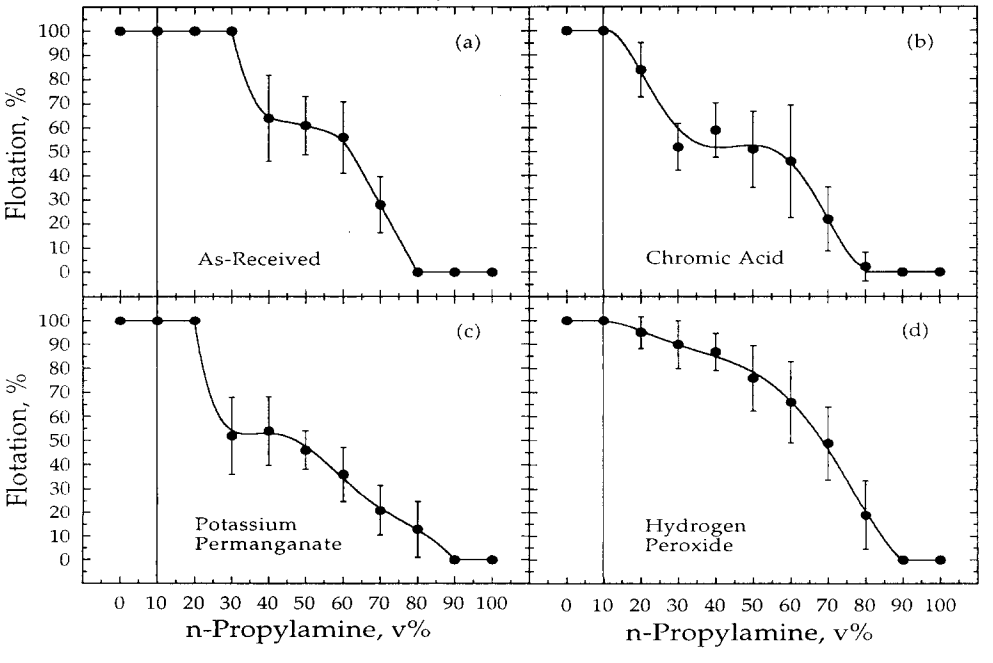

Figure 6 Flotation as a function of n-PA concentration for fibres: (a) as-received; (b) chromic acid etched; (c) $KMnO_4$ etched; (d) H_2O_2 etched

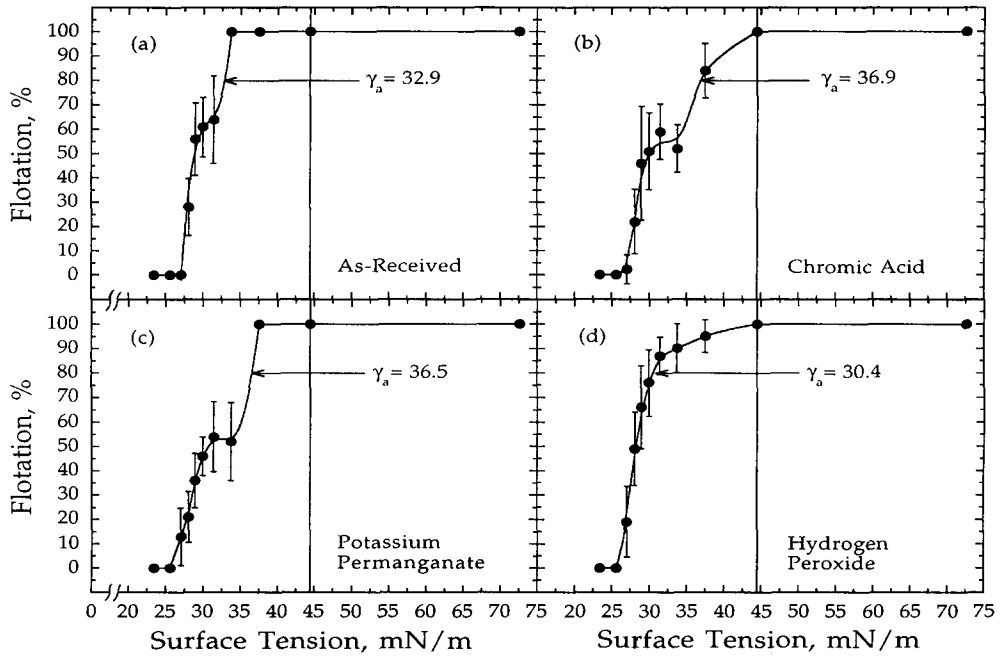

Figure 7 Flotation as a function of liquid surface tension for fibres: (a) as-received; (b) chromic acid etched; (c) $KMnO_4$ etched; (d) H_2O_2 etched

The ideally sharp float/sink transition is far from being realized in these flotation diagrams. The shape of the flotation diagrams may be somewhat distorted by the non-linear relationship between surface tension and nPA content. The experimentally determined relationship between nPA content and surface tension in *Figure 5* can be used to plot flotation in terms of surface tension. The flotation diagrams in *Figures 7a–d* correspond to those in *Figures 6a–d*, respectively. The float/sink transitions seen in *Figures 7a–d* are more sharply defined than those seen in *Figures 6a–d*. The plateaux in the as-received, chromic acid etched and $KMnO_4$ etched fibres are not as dominant a feature in *Figures 7a–c*, respectively, but still distinguish those fibres from the H_2O_2 etched fibres in *Figure 7d*.

The surface tension at which the fibres begin to sink, the initiation of the float/sink transition, can also be used to distinguish between the different fibres. The transition begins at higher surface tension values for chromic acid etched and H_2O_2 etched fibres and at a significantly lower value for the as-received fibres. The transition initiation for the $KMnO_4$ etched fibres lies between those of the as-received and chromic acid etched fibres.

UHMW-PE fibre wettability

The wettability and the float/sink transition are affected by two different aspects of the fibre surface. An increase in roughness can yield an increase in the apparent surface tension[5]. The etching process exposes the UHMW-PE fibrillar structure and greatly increases surface roughness. Fibres with increased roughness will sink at higher apparent surface tensions. The initiation of the float/sink transition occurs at a lower surface tension for the smooth as-received fibres and at a higher surface tension for the rougher etched fibres.

The surface tension is also increased by the introduction of polar groups, such as oxygen, to the fibre surface[5]. The increase in hydrogen bonding at an oxidized polymer surface may be especially significant with the strongly hydrogen bonding nPA used in the flotation experiments. The as-received, chromic acid etched and $KMnO_4$ etched fibres with relatively high surface oxygen contents all display a plateau in their flotation diagrams. The oxygen-rich fibre surface may preferentially associate with nPA molecules through strong hydrogen bonding. A low surface tension sheath rich in nPA may be formed around the fibre through preferential hydrogen bonding.

The lower surface tension sheath solution would better wet the fibres than the higher surface tension bulk solution. The enhanced wetting would result in flotation that reflects the sheath solution, and not the bulk solution. The sheath solution composition would reflect the oxygen content of the fibre surface and remain constant over a range of bulk solution compositions. The plateau in the flotation diagrams could result from the formation of a nPA-rich sheath at low nPA concentrations. The plateau in flotation would end once the nPa concentration in the bulk is greater than that of the sheath formed around the polar surface of the fibre.

The effects of etching on both the surface roughness and surface oxygen seem to be reflected in the flotation diagrams. Ascribing a quantitative surface tension to these fibres from the flotation diagrams, however, is not straightforward. There are numerous assumptions made in deriving the theory describing the float/sink transitions. Moreover, practically, the width and shapes of the flotation diagrams make it difficult to find a common point for comparison. The surface tension should reflect both the effects of surface roughness and surface oxygen on the fibre. The roughness seems to be reflected in the initiation of the float/sink transition while the oxygen seems to be reflected in the flotation plateau. The liquid surface tension at 80% flotation, between the initial decrease and the plateau, was chosen as the point from which to derive the solid surface tension. The liquid surface tension at 80% flotation can be defined as the solid's apparent surface tension from flotation (γ_a).

The apparent surface tensions of the various fibres from *Figure 7* are listed in *Table 2* and plotted in *Figure 8*. *Figure 8* also includes the surface oxygen

Table 2 Apparent surface tension of UHMW-PE fibres

Etch	Time (h)	γ_a (mN m^{-1})
None	–	32.9
$K_2Cr_2O_7$	4	36.9
$KMnO_4$	4	36.5
H_2O_2	4	30.4

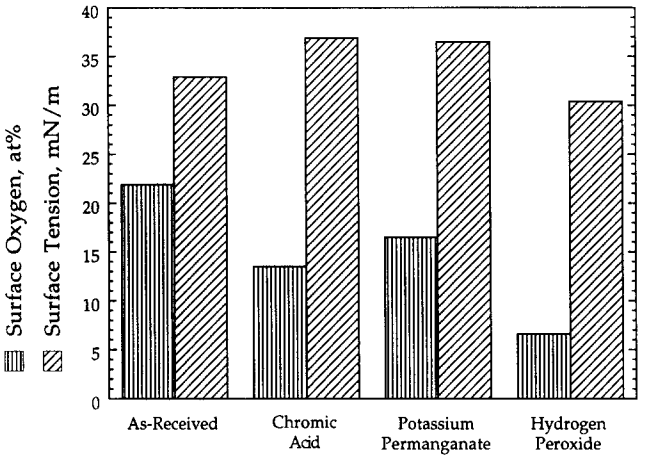

Figure 8 Apparent surface tension and surface oxygen content for as-received and etched fibres

content from *Table 1*. The lack of direct correlation between oxygen content and apparent surface tension emphasizes the importance of the surface roughness factor. The chromic acid etched (37 mN m^{-1}) and $KMnO_4$ etched (37 mN m^{-1}) fibres have rough and oxygen-rich surfaces and the greatest wettability. The H_2O_2 etched (30 mN m^{-1}) and as-received (33 mN m^{-1}) fibres have a lower apparent surface tension reflecting a low surface oxygen content and a smooth surface, respectively.

CONCLUSIONS

The analytical solutions to the net force balance for a cylinder floating on a liquid medium provide the conditions for a float/sink transition for both larger and smaller cylinders. UHMW-PE fibres, which fit into the smaller cylinder category, undergo this transition when they are enveloped by the flotation medium (water and nPA). This envelopment was taken to occur when $\phi = 180°$ and $\theta = 0°$. The flotation diagram can be used to characterize the effects of surface roughness and surface oxidation.

The significant surface oxygen content of the as-received, chromic acid etched or $KMnO_4$ etched fibres yields a plateau in the flotation diagram. The increase in surface roughness for the etched fibres is reflected in the initation of the float/sink transition at higher surface tensions. The surface tension at 80% flotation has been used to reflect both the effects of roughness and oxygen on fibre wettability. The apparent surface tension of the rough and oxygen-rich chromic acid etched (37 mN m^{-1}) and $KMnO_4$ (37 mN m^{-1}) etched fibres is greater than those of the H_2O_2 etched (30 mN m^{-1}) and as-received (33 mN m^{-1}) fibres reflecting a low surface oxygen content and a smooth surface, respectively.

ACKNOWLEDGEMENT

The authors wish to thank Professor Avi Marmur of the Department of Chemical Engineering, Technion, for his suggesting the flotation technique and his insightful discussions and assistance throughout.

REFERENCES

1 Prevorsek, D. C., Chin, H. B., Kwon, Y. D. and Field, J. E. *J. Appl. Polym. Sci., Appl. Polym. Symp.* 1991, **47**, 45
2 Silverstein, M. S. and Breuer, O. *J. Mater. Sci.* in press
3 Tissington, B., Pollard, G. and Ward, I. M. *J. Mater. Sci.* 1991, **26**, 82
4 Ladizesky, N. H. and Ward, I. M. *Composites Sci. Technol.* 1986, **26**, 129
5 Kinloch, A. J. 'Adhesion and Adhesives', Chapman and Hall, New York, 1987
6 Silverstein, M. S., Breuer, O. and Dodiuk, H. in preparation
7 Silverstein, M. S. and Breuer, O. *J. Mater. Sci.* in press
8 Wagner, H. D. *J. Appl. Phys.* 1990, **67**, 1352
9 Gilbert, A. H., Goldstein, B. and Marom, G. *Composites* 1990, **21**, 408
10 Nardin, M. and Ward, I. M. *Mater. Sci. Technol.* 1987, **3**, 814
11 Marmur, A., Chen, W. and Zografi, G. *J. Colloid Interface Sci.* 1986, **113**, 114
12 Rapacchietta, A. V., Neumann, A. W. and Omenyi, S. N. *J. Colloid Interface Sci.* 1977, **59**, 541